Development of an integrated model framework for multi-air-pollutant exposure assessments in high-density cities

Zhiyuan Li[1,2], Kin-Fai Ho[3], Harry Fung Lee[4], Steve Hung Lam Yim[5,6,7,*]

[1]School of Public Health (Shenzhen), Sun Yat-sen University, Guangzhou 510275, China
[2]Institute of Environment, Energy and Sustainability, The Chinese University of Hong Kong, Shatin, N.T., Hong Kong, China
[3]The Jockey Club School of Public Health and Primary Care, The Chinese University of Hong Kong, Shatin, N.T., Hong Kong, China
[4]Department of Geography and Resource Management, The Chinese University of Hong Kong, Shatin, N.T., Hong Kong, China
[5]Asian School of the Environment, Nanyang Technological University, Singapore
[6]Lee Kong Chian School of Medicine, Nanyang Technological University, Singapore
[7]Earth Observatory of Singapore, Nanyang Technological University, Singapore

Correspondence to: Steve Hung Lam Yim (steve.yim@ntu.edu.sg)

Abstract. Exposure models for some criteria air pollutants have been intensively developed in past research; multi-air-pollutant exposure models, especially for particulate chemical species, have been however overlooked in Asia. Lack of an integrated model framework to calculate multi-air-pollutant exposure hinders the combined exposure assessment and the corresponding health assessment. This work applied the land-use regression (LUR) approach to develop an integrated model framework to estimate 2017 annual-average exposures of four major PM_{10} chemical species as well as four criteria air pollutants of PM_{10}, $PM_{2.5}$, NO_2, and O_3 in a typical high-rise and high-density Asian city (Hong Kong, China). Our integrated multi-air-pollutant exposure model framework is capable of explaining 91–97% of the variability of measured air pollutant concentration, with the leave-one-out cross-validation R^2 values ranging from 0.73 to 0.93. Using the model framework, the spatial distribution of the concentration of various air pollutants at a spatial resolution of 500 m was generated. The LUR model-derived spatial distribution maps revealed weak to moderate spatial correlations between the PM_{10} chemical species and the criteria air pollutants, which may help to distinguish their independent chronic health effects. In addition, further improvements in the development of air pollution exposure models are discussed. This study proposes an integrated model framework for estimating multi-air-pollutant exposure in high-density and high-rise urban areas, serving an important tool for combined exposure assessment in epidemiological studies.

1 Introduction

Ambient air pollution has been identified as one of the most important health risk factors, contributing to premature deaths and disabilities worldwide (Bowe et al., 2018; Burnett et al., 2018; HEI, 2019; Yim et al., 2019; Yim et al., 2022). In 2017, air pollution is ranked as the fifth among all-mortality risk factors globally, accounting for nearly 5 million premature deaths (HEI, 2019). Ambient $PM_{2.5}$ (particles of aerodynamic diameter less than or equal to 2.5 μm) was associated with 2.9 million premature deaths, and ozone (O_3) accounted for approximately 0.5 million premature deaths in 2017 (HEI, 2019). Numerous previous epidemiological studies have documented good evidence of the positive association between air pollution exposures and various types of health-effect endpoints, such as stroke, heart diseases, asthma, and lung cancer (Crouse et al., 2015; Fan et al., 2018; Renzi et al., 2019; Wang et al., 2017; Xue et al., 2021). For example, Renzi et al. (2019) estimated that there were increases of 0.8%, 0.9%, and 1.4% in non-accidental, cardiovascular, and respiratory mortality, respectively, for every 1 μg/m^3 increase in annual-average PM_{10} (particles of aerodynamic diameter less than or equal to 10 μm) concentration in the Latium region of Italy during 2006–2012.

Polluted air mass contains a complex mixture of toxic particles and various gas-phase pollutants. Health effects from air pollution are consequences from combined exposure to air pollution mixtures (Coker et al., 2016; Levy et al., 2014; Stafoggia et al., 2017; Wang et al., 2022a; Xue et al., 2021; Yim et al., 2022). For instance, Wang et al. (2022a) found that PM_{10} and O_3 dominated the health effects of air pollution mixtures on obstructive sleep apnea, a common sleep-related breathing disorder, in a cross-sectional study in Beijing, China. Up until now, most epidemiological studies targeting at air pollution and various health endpoints have typically focused on estimating the adverse health effects associated with exposure to a single pollutant (or pollutant category) mainly due to the difficulties of conducting a multi-air-pollutant exposure assessment (Dominici et al., 2010; Wang et al., 2022b). In recent years, the scientific community has been moving toward a multi-air-pollutant concept to quantify the health hazards of air pollution mixtures as a whole (Chen et al., 2020a; Dominici et al., 2010; Mauderly et al., 2010; Vedal et al., 2010; Xue et al., 2021; Yim et al., 2022). To achieve this target, we need to work on multi-air-pollutant exposure assessment to support the corresponding health-related studies (Billionnet et al., 2012; Mauderly et al., 2010).

In order to assess health effects of air pollution mixture, an integrated model framework is urgently needed to estimate exposures to multiple air pollutants. However, the available exposure assessment studies typically focused on one or several criteria air pollutants, mainly traffic-related air pollutants of $PM_{2.5}$ and nitrogen dioxide (NO_2) (Cai et al., 2020; Cordioli et al., 2017; Hoek et al., 2008; Jin et al., 2019; Luminati et al., 2021; Ross et al., 2007; Xu et al., 2019). For example, Jin et al. (2019) estimated annual average exposures to $PM_{2.5}$ and NO_2 in Lanzhou, China, with R^2 values at 0.77 and 0.71, respectively. In addition, Luminati et al. (2021) developed the NO_2 exposure model in Sao Paulo, Brazil using the land-use regression (LUR) approach. Apart from these criteria air pollutants, other air pollutants, such as the chemical species of ambient particles, should also be studied, given their significant but independent toxicity and health risk (Li et al., 2022;

Rappazzo et al., 2021; Requia et al., 2019; Wang et al., 2022b). To the best of our knowledge, none of these previous studies has comprehensively evaluated the spatial heterogeneity among a large set of air pollutants (e.g., particles and their chemical species, and gaseous pollutants) (Cai et al., 2020; Hoek et al., 2008; Li et al., 2021). Thus, it is essential to explore the

65 establishment of an integrated multi-air-pollutant model framework to support epidemiological studies to isolate the health effects of multiple air pollutants.

The major objective of this study was to develop an integrated model framework for multi-air-pollutant exposure assessments in high-density and high-rise cities. The case of Hong Kong was illustrated to estimate annual-average exposures of major chemical species of ambient PM_{10} as well as ambient PM_{10}, $PM_{2.5}$, NO_2, and O_3. Materials and methods,

70 including the development and application of an integrated multi-air-pollutant model framework in Hong Kong, are described in Section 2. Section 3 presents the established multi-air-pollutant models and the spatial distribution maps of targeted air pollutants derived from the established models. The discussion and implications are provided in Section 4.

2 Materials and methods

As shown in Figure 1, we developed an integrated model framework for establishing multi-air-pollutant exposure models

75 with two major modules of particulate matters (PM module) and gaseous pollutants (GAS module). The PM and GAS modules were separated because the measurement and LUR modelling of PM species and gaseous pollutants are largely different in terms of measurement techniques, the number of required measurement sites, and selected predictor variables, etc. The integrated model framework handles the input datasets required for the PM and GAS modules and develops the LUR model for each air pollutant independently. The LUR models and the corresponding spatial distribution maps within

80 each module can be used to further validate the LUR models and the corresponding spatial distribution maps under the same or another module (Li et al., 2021). For instance, in high-density cities, the spatial distribution of O_3 shows a generally opposite spatial variability compared with traffic-related air pollutants because of the NO_x reaction with O_3. The established LUR models of the PM and GAS modules were used for the assessment of exposure in epidemiological studies. In the present study, the PM module includes the LUR models for different sizes of PM and its chemical components, whereas the

85 GAS module includes the LUR models for two typical gaseous pollutants of NO_2 and O_3. The included air pollutants vary depending on the data availability when the proposed integrated model framework is applied in other cities.

2.1 Study area

Hong Kong (latitude 22°08'N and 22°35'N, longitude 113°49'E and 114°31'E) is a mountainous high-density and high-rise city situated at the southeast coast of the Pearl River Delta (PRD) region, China (Yim et al., 2009). Hong Kong has a total

90 land area of about 1100 km^2, of which 24% is built-up area. It has a population of over 7 million, and the population density of 6,690 people per square kilometer is among the highest in the world (Li et al., 2018). Hong Kong is characterized by cool and dry winters with an average temperature of 19 °C, and hot and humid summers with afternoon temperatures often above

31 °C and night temperatures around 26 °C (HKO, 2020). Hong Kong is typically influenced by the transboundary air pollution issue, when polluted air masses are transported from the PRD region and beyond to the region in winter (Lee et al.,

95   2017; Li et al., 2020; Yim, 2020). The traffic density in Hong Kong is among the highest in the world, with 839,882 registered vehicles on 2100 km of road in 2017 (HKTD, 2020). Therefore, the traffic emission from different types of vehicles is another important source of air pollution in Hong Kong (Li et al., 2022).

2.2 Air pollution monitoring data

The Hong Kong air quality monitoring network provides good representation because the locations of air quality monitoring

100 stations (AQMSs) were chosen with reference to international guidelines and with practical consideration for the localized city characteristics (Figure S1 in the Supplementary Information). The environmental characteristics of the AQMSs are summarized in Table S1. The daily average concentration data of PM_{10}, $PM_{2.5}$, NO_2, and O_3, measured at 16 AQMSs, operated by the Hong Kong Environmental Protection Department (HKEPD), were collected from 1 January 2017 to 31 December 2017 (https://cd.epic.epd.gov.hk/EPICDI/air/station/, last accessed on September 2023). These AQMSs are

105 generally diverse and representative, ranging from rural stations under a limited influence of anthropogenic emissions to traffic stations near the major roads in Hong Kong. PM_{10} and $PM_{2.5}$ are measured continuously by automatic monitors, while the Opsis AR 500 system and the T-API 400 system are used to measure NO_2 and O_3 concentration, respectively (HKEPD, 2018). The details for the list of equipment for measurement of air pollutant concentration as well as the quality control and assurance procedures are documented in HKEPD (2018). All of the air pollutant concentration data had at least 345 daily

110 values, which represents a relatively complete set of data. Due to data availability, the 2017 annual-average concentration of these air pollutants was estimated for development of the LUR models using collected daily air pollutant concentration data. In addition, the annual-average concentration of four major PM_{10} chemical species, including total carbon (TC), nitrate (NO_3^-), sulfate (SO_4^{2-}), and cadmium (Cd), at 10 AQMSs was collected from the air quality reports of the HKEPD (https://www.aqhi.gov.hk/en/download/air-quality-reportse469.html?showall=&start=1, last accessed on September 2023)

115 for development of the LUR models.

2.3 Potential predictor variables

All of the potential predictor variables with their corresponding buffer sizes and data sources are summarized in Table S2 and Figure S2. Meteorological variables (i.e., wind speed, wind direction, relative humidity, and temperature) were collected from nearby weather stations operated by the Hong Kong Observatory (https://www.hko.gov.hk/en/index.html, last accessed

120 on September 2023). In addition, five categories of geospatial predictor variables including land use, road networks with traffic volume information, population density data, topography, and urban/building morphology were collected from various databases (Table S2). The ArcGIS software, version 10.6 (ESRI Inc., Redlands, CA, USA) was used to process these datasets. The land-use type was classified into 10 main categories and 27 subcategories. The 10 main categories of land use included residential, commercial, industrial, institutional/open space, transportation, other urban or built-up land, agriculture,

125 woodland/shrubland/grassland/wetland, barren land, and water bodies (https://www.pland.gov.hk/pland_en/info_serv/open_data/landu/index.html, last accessed on September 2023). The traffic volume data for different vehicle types were provided by the Hong Kong Transport Department (https://data.gov.hk/en-data/dataset/hk-td-tis_15-road-network-v2, last accessed on September 2023). Seven vehicle types, including private cars, non-franchised buses, light goods vehicles, franchised buses, medium and heavy goods vehicles, taxis, and public light buses

130 were counted. Values of these geospatial variables in buffer sizes of 50 m, 100 m, 300 m, 500 m, 700 m, 1000 m, 2000 m, 3000 m, 4000m, and 5000 m around the AQMSs were estimated as the potential predictor variables using ArcGIS buffer analysis. The geo-locations (longitude and latitude) were also adopted because they can reveal a north-south or west-east variability gradient of air pollutant concentrations which are not captured by the selected predictor variables in the model (Huang et al., 2017). The geographical coordinate information for each station was obtained from the HKEPD.

135 **2.4 Development of multi-air-pollutant exposure models**

The LUR approach is based on the principle that air pollutant concentration at a given location depends on the environmental features (e.g., land-use types, traffic volume, meteorological conditions, etc.) of the surrounding area (Supplementary Text S1) (Li et al., 2022; Lu et al., 2020; Meng et al., 2015; Naughton et al., 2018; Wu et al., 2017). The supervised forward linear regression method was utilized to conduct the LUR modelling of multiple air pollutants (Eeftens et al., 2012; Eeftens et al.,

140 2016; Huang et al., 2017; Jin et al., 2019; Liu et al., 2016; Saha et al., 2020). The method computed the direction of effect for a predictor variable to reflect the effect of the predictor variable on air pollutant concentration. While the direction of effect can be positive or negative, the method first judged the direction of effect for each type of predictor variable based on the currently known relationship between the predictor variable and the corresponding air pollutant. As a secondary pollutant, O_3 is involved in many complex chemical reactions and the expected directions of the predictor effects were not as

145 clear as for the other air pollutants (Li et al., 2022; Wolf et al., 2017), and O_3 was thus considered carefully in the process. Using the full dataset, we ranked all the predictor variables based on their adjusted explained variance (adjusted R^2) with air pollutant concentration. The predictor variable with the highest adjusted R^2 was selected to be included in the model if the direction of effect was consistent with our judgement. We then evaluated which of the remaining predictor variables further improved the adjusted R^2 of the LUR model, and selected the one giving the largest gain in the adjusted R^2 of the model and

150 with the right direction of effect. Subsequent predictor variables were not selected if they changed the direction of effect of one of the previously included predictor variables. This process continued to be proceeded until there were no more predictor variables with the right direction of effect, which added at least 1% to the adjusted R^2 of the previous LUR model. Finally, the predictor variables with a P-value above 0.10 were removed from the LUR model. If the variance inflation factor (VIF), which measures the severity of multicollinearity in regression analysis, was higher than 5.0, the predictor variable with the

155 highest VIF was removed and the model was re-established (Gulliver et al., 2018; Hsu et al., 2018; Jones et al., 2020; Ma et al., 2019; Zhang et al., 2015). Due to this procedure, the included predictor variables may obscure the potential influence of others.

The spatial autocorrelation (Moran's I) tool measures spatial autocorrelation using both feature locations and feature values simultaneously. Meanwhile, z-score and P-values were calculated to evaluate the significance of Moran's I value. z-score values are standard deviations, whereas the Moran's I index is bounded by -1.0 and 1.0. When the z-score or P-value indicates statistical significance, a positive Moran's I index value indicates tendency towards clustering, whereas a negative Moran's I index value indicates tendency towards dispersion (Cordioli et al., 2017; Luminati et al., 2021). Moran's I index and the corresponding z-score and P-value on concentration residuals of the final LUR models were quantified using ArcGIS software to evaluate their spatial autocorrelation. Leave-one-out cross-validation (LOOCV) was used to evaluate the predictive ability of the established LUR model to a new dataset (Ma et al., 2019; Wu et al., 2017). In brief, each station was withheld from the model sequentially, whereas the remaining stations were used to establish the model. The concentration at the withheld station was estimated using the established model in each iteration. The procedure was repeated until all the stations have been predicted once (Eeftens et al., 2016; Ji et al., 2019; Wolf et al., 2017). A number of statistical parameters of the linear regression between measured and predicted concentration of the omitted stations, including R^2, root mean squared error (RMSE), were used to validate the performance. The statistical analysis was performed using R statistical software, version 3.5.2 for Windows (R Foundation for Statistical Computing, Vienna, Austria).

2.5 Spatial mapping of studied air pollutants

The spatial distribution maps of predicted annual-average concentration of PM_{10} and its chemical species, $PM_{2.5}$, NO_2, and O_3 were generated based on the final LUR models, following the typical procedures of previous studies (Cai et al., 2020; Huang et al., 2017; Xu et al., 2019). A spatial resolution of 500 m ×500 m was adopted here due to the spatial resolution of most predictor variables is at several hundred meters resolution. The study area of Hong Kong was divided into grids at the spatial resolution of 500 m, and the pollutant concentration at the centroid of each grid was estimated. Finally, the pollution distribution maps were generated using the predicted concentration values (Henderson et al., 2007). The LUR model estimated concentration of the studied air pollutants in the eighteen districts of Hong Kong was summarized and compared.

3 Results

3.1 Air pollutant measurements

The measurements at the AQMSs show that the annual-average PM_{10} and $PM_{2.5}$ concentration varied between 30.9–45.7 $\mu g/m^3$ and 18.4–31.2 $\mu g/m^3$, respectively (Figure S3), which were higher than the air quality guideline (AQG) for PM_{10} (15.0 $\mu g/m^3$) and $PM_{2.5}$ (5.0 $\mu g/m^3$) proposed by the World Health Organization (WHO) (WHO, 2021). PM_{10} TC, PM_{10} NO_3^-, PM_{10} SO_4^{2-}, and PM_{10} Cd had annual-average concentration of 4511–9019 ng/m^3, 2920–4642 ng/m^3, 6713–7525 ng/m^3, and 0.58–0.72 ng/m^3, respectively. The annual-average NO_2 concentration was from 9.70 $\mu g/m^3$ to 197.0 $\mu g/m^3$, which were generally higher than the WHO NO_2 AQG of 10 $\mu g/m^3$ (WHO, 2021). The annual-average O_3 concentration ranged from 17.8 $\mu g/m^3$ to 73.9 $\mu g/m^3$ in Hong Kong (Figure S3).

3.2 Multi-air-pollutant exposure models

190   The established annual-average LUR models for ambient PM_{10}, $PM_{2.5}$, NO_2, O_3, and four major PM_{10} chemical species are shown in Table S3. Overall, the established LUR models achieved relatively good predictive accuracy (Table S3, Figures 2, S4, S5, S6, and S7), with training and LOOCV R^2 values ranging between 0.91–0.97 and 0.73–0.93, respectively. The prediction error fractions of the LUR models ranged between -5.9%–7.0%, -6.1%–14%, -4.5%–7.3%, -1.1%–1.2%, -2.3%–3.8%, -8.1%–8.6%, -24%–25%, and -13%–27%, respectively, for PM_{10}, PM_{10} TC, PM_{10} NO_3^-, PM_{10} SO_4^{2-}, PM_{10} Cd, $PM_{2.5}$,

195   NO_2, and O_3 (Figure 2). There were two to five predictor variables included in the final models, which is typically within the range of the number of predictor variables in previous studies (Cai et al., 2020; Henderson et al., 2007; Li et al., 2022; Meng et al., 2016; Miri et al., 2019). The selection of these predictor variables was driven by the emission sources of the air pollutants, the dispersion and transport condition, and the influence of transboundary air pollution in Hong Kong. The selected predictor variables included traffic emission-related variables, different land-use types (e.g., the industrial land),

200   population density, urban morphology (e.g., the canyon height), and geographical locations (Table S3).

Five predictor variables were entered into the PM_{10} LUR model, including the number of private cars in a buffer size of 100 m, the area of buildings within a 100-m buffer, the area of residential land in a buffer size of 100 m, the area of industrial land within a 3000-m buffer, and the area of urban green space in a buffer size of 4000 m. Among these predictor variables, only the urban green space had a negative direction of effect. The R^2 and LOOCV R^2 values were 0.92 and 0.77,

205   respectively, representing a remarkable PM_{10} concentration prediction (Table S3). Residual spatial autocorrelation analysis of the PM_{10} LUR model is shown in Figure S8. The z-score is 0.399, which means that the model residuals are not spatially correlated, confirming that the PM_{10} LUR model was reasonably established.

For the LUR models of PM_{10} chemical species, two to three predictor variables were selected finally. As expected, the traffic-related predictor variables and urban/building morphology-related parameters dominated the variability of the four

210   chemical species, because the PM_{10} chemical species in the city were mainly influenced by vehicular emissions and urban form patterns (Hsu et al., 2018; Li et al., 2022). For example, the Cd LUR model included the area of transportation land in a buffer size of 2000 m, latitude, and the average canyon height within a 300-m buffer. The R^2 and LOOCV R^2 values ranged between 0.92–0.97 and 0.73–0.92, respectively, suggesting a relatively high predictive accuracy (Table S3). The assumption of spatial error independence was confirmed with z-score values at -0.249, 0.453, -0.504, and -0.843 for PM_{10} TC, PM_{10}

215   NO_3^-, PM_{10} SO_4^{2-}, and PM_{10} Cd, respectively (Figure S8).

The $PM_{2.5}$ LUR model included five predictor variables, namely the number of light-duty vehicles in a buffer size of 500 m, the area of urban green space within a 4000-m buffer, the area of residential land in a buffer size of 300 m, the area of buildings within a 50-m buffer, and the maximum building height in a buffer size of 100 m. Four of these variables were the same as those in the PM_{10} LUR model, even though the buffer sizes varied. The R^2 and LOOCV R^2 values and the z-score

values all confirmed that the PM$_{2.5}$ LUR model was reasonably established with an acceptable statistical performance (Table S3 and Figure S8).

The predictor variables included in the NO$_2$ LUR model were the number of total vehicles within a 500-m buffer, the number of people in a buffer size of 100 m, and the area of industrial land within a 1000-m buffer. These predictor variables all had a positive effect on NO$_2$ concentration, as evidenced by the positive regression slope values. The R^2 and LOOCV R^2 values were 0.96 and 0.93, respectively, indicating the relatively good prediction performance of the model (Table S3). The model residuals were spatially independent, with a z-score value at 0.935 (Figure S8).

The predictor variables included in the O$_3$ LUR model were the number of total vehicles in a buffer size of 700 m, longitude, and the area of urban green space within a 300-m buffer. The predictor variable of vehicles had a negative effect on O$_3$ concentration. This negative effect reflects the titration of O$_3$ in urban areas with a large amount of NO and NO2 emitted by traffic (Han et al. 2023). Longitude has a positive effect on O$_3$ concentration, suggesting the influence of regional transported air masses. A LUR study in Nanjing, China also included longitude in the final O$_3$ model (Huang et al., 2017). Urban green space had a positive effect on O$_3$ concentration, which is probably due to biogenic volatile organic compounds as the precursors of ozone formation (Ma et al., 2021; Ren et al., 2017). The R^2 and LOOCV R^2 values were 0.92 and 0.87, respectively, showing the relatively high predictive accuracy of the model (Table S3). The z-score (1.186) of the residual spatial autocorrelation analysis indicates that the O$_3$ LUR model was well explained by the included predictor variables, with spatially independent model residuals (Figure S8).

3.3 Spatial distribution maps

The spatial distribution maps of multiple air pollutants derived from established LUR models are shown in Figure 3, whereas Table S4 shows the statistical description of the estimated air pollutant concentration. The PM$_{10}$, PM$_{2.5}$, and NO$_2$ LUR models included several predictor variables (e.g., the number of medium and heavy-duty vehicles in a buffer size of 500 m) representing vehicular emissions (Table S3). Thus, the concentration of PM$_{10}$, PM$_{2.5}$, and NO$_2$ is largely affected by the traffic emissions in Hong Kong, with higher concentration estimated along the road network. In addition, the relatively higher concentration of PM$_{10}$, PM$_{2.5}$, and NO$_2$ was estimated in areas with the high population density (e.g., the northern part of Hong Kong island, the Kowloon City district, and the Yau Tsim Mong district). PM$_{10}$ and PM$_{2.5}$ had moderate positive corrections with NO$_2$, with Pearson correlation coefficient (PCC) values at 0.570 and 0.696, respectively (Table 1). Consistent with Li et al. (2022), the LUR model-derived concentration of PM$_{10}$ TC, PM$_{10}$ NO$_3^-$, and PM$_{10}$ SO$_4^{2-}$ was relatively higher at developed urban areas and along major roads. In contrast to this, the spatial distribution of PM$_{10}$ Cd showed a north–south gradient, with relatively higher concentration in the northern part and relatively lower concentration in the southern part. These PM$_{10}$ chemical species only had weak to moderate positive correlations with PM$_{10}$ mass, with PCC values ranging from 0.189 to 0.589 (Table 1). For O$_3$, there was an increasing trend from west to east, suggesting the

influence of transboundary pollution on the spatial distribution pattern. In addition, O_3 concentration was largely affected by traffic emissions, with lower concentration estimated along major roads compared with other areas. Due to nitric oxide titration (Han et al., 2023), O_3 concentration was generally negatively correlated by various degree with PM_{10}, PM_{10} chemical species, $PM_{2.5}$, and NO_2 (Table 1).

255   The spatial patterns of the studied air pollutants varied largely among the districts (Table S5 and Figure S9). As shown by the three example districts in Figure 4, the Yuen Long district had relatively high concentration of PM_{10}, PM_{10} species, and $PM_{2.5}$, and moderate concentration of NO_2 and O_3. For the Yau Tsim Mong district, the PM_{10}, PM_{10} species, $PM_{2.5}$, and NO_2 concentration was relatively high, whereas the O_3 concentration was quite low. In contrast to this, the Sai Kung district had quite high concentration of O_3 but relatively low concentration of other studied air pollutants.

4 Discussion and implications

High-density cities usually have spare air quality monitoring stations. This discrepancy clearly highlighted the need to develop LUR models for the spatial mapping of air pollution in high-density cities. This work developed an integrated model framework for a high-density city based on the air quality data collected at the sparse monitoring stations. Following the proposed integrated model framework, we established multi-air-pollutant exposure models for four major PM_{10} chemical
265   species as well as four criteria air pollutants in Hong Kong using the LUR model approach (Table S3). Similar to other LUR model studies, one limitation of this study is typically the limited number of monitoring stations. It should be noted that the adequacy of monitoring should not be determined by number of stations alone. This study therefore performed detailed evaluations to examine the adequacy. In the GAS module, the established NO_2 and O_3 exposure models had R^2 values at 0.96 and 0.92, respectively, which are similar with previous studies. In the PM module, our PM_{10} and $PM_{2.5}$ exposure models
270   achieved remarkable predictive accuracy, comparable with or higher than those of the traditional LUR studies (Tables 2 and S3; Supplementary Text S2). Following our previous study of Li et al. (2021), in the PM module, we established LUR exposure models of PM_{10} TC, PM_{10} NO_3^-, PM_{10} SO_4^{2-}, and PM_{10} Cd, with model R^2 values higher than 0.92 (Table S3). The detailed evaluation results have proved that our models had promising performance and are capable of reflecting the air quality characteristics of the city. Therefore, our models are considered as sufficient for the scope of this study. Certainty, it
275   is strongly recommended to carry out a further study using different modelling methods (e.g., machine learning) when more data are available with at a finer temporal resolution or collected from a larger number of monitoring stations.

This research work aimed to contribute to the research area of exposure assessment through providing new opportunities to distinguish the independent associations between combined exposure to multiple air pollutants (i.e., PM_{10}, PM_{10} TC, PM_{10} NO_3^-, PM_{10} SO_4^{2-}, PM_{10} Cd, $PM_{2.5}$, NO_2, and O_3) and chronic health effects. For example, the finding of weak to moderate
280   spatial correlation between PM_{10} and its chemical species may enable epidemiological studies to separate the chronic health effects of PM_{10} chemical species from the total mass. In addition, the spatial variation of air pollution can be used for hotspot

identification for air quality management and exposure assessment in epidemiological studies using the geospatial locations of the subjects (Crouse et al., 2015; Jones et al., 2020; Li et al., 2021). The major explanation for the spatial differences in concentration of multiple air pollutants was the differences in their emission sources (Cai et al., 2020; Jin et al., 2019; Levy et al., 2014; Wu et al., 2017). For instance, $PM_{2.5}$ and NO_2 are more linked to traffic and industrial emissions in developed urban areas, while relatively high O_3 concentration in rural areas is formed through complex chemical reactions between biogenic volatile organic compounds and nitrogen oxides (Table S3 and Figure 3). The results highlight that the synergistic control of multiple emission sources and key precursors is urgently needed for the joint control of multiple air pollutants (Saha et al., 2020; Yim et al., 2019). For instance, the Hong Kong government has spent tremendous efforts on the reduction of vehicular emissions over the past two decades, which successfully reduced traffic-related air pollutants like $PM_{2.5}$ and NO_2. However, as revealed by the present study and previous studies (HKEPD, 2022; Zeng et al., 2022), O_3 pollution has become an emerging issue, especially in rural areas of Hong Kong. The relationship between the control of vehicular emissions and O_3 pollution is complex (Song et al., 2023; Zeng et al., 2022). In Hong Kong, NO_x reductions from the control of vehicular emissions may lead to an increase in the levels of oxidants, and then cause a net O_3 production. It is suggested that the control of volatile organic compounds should be implemented to better mitigate O_3 pollution in HK (Zeng et al., 2022). This highlights the importance to simulate multiple air pollutants together during exposure assessments. In addition, more research should be conducted to understand the complex and varying interaction of emission sources, pollutant sensitivity to precursors, and air quality in a city to formulate more effective and specific air quality management policies.

The development and applicability of exposure models depends on the focus of the air pollution epidemiological studies, which either focus on long-term or short-term or even acute exposure. To the best of our knowledge, the annual or long-term LUR exposure models have been widely adopted in providing long-term exposure estimates for health studies (Chen et al., 2021; Wang et al., 2020b). Meanwhile, considering the requirement for high spatial-resolution and short-term acute exposure assessment, it is recommended that more studies are conducted to establish high spatiotemporal-resolution exposure models when detailed measurement data are available. Indeed, several recent studies have explored the possibility of estimating high spatiotemporal-resolution air pollution exposure models using the spatiotemporal statistical modelling approach (Lu et al., 2020; Masiol et al., 2018). In addition, in future studies, a multi-dimensional and multi-air-pollutant exposure modelling approach is recommended, for instance, by combining spatiotemporal statistical modelling with atmospheric chemistry knowledge, with the particulate chemical species and their toxicity and volatile organic compounds being modelled (Brokamp et al., 2017; Chen et al., 2020b; Lu et al., 2020). In addition, the vertical distribution of air pollutants should be measured and modelled to combine with spatiotemporal exposure models to reveal the vertical variability of population exposure to air pollution (Eeftens et al., 2019; Ho et al., 2015; Jin et al., 2019). Moreover, most previous air pollution exposure assessment studies and the current work have focused on ambient air quality, but it is strongly recommended that more research efforts should be made toward developing prediction models of air pollutant concentration in indoor environments (e.g., residential households) for more accurate exposure estimates (Tang et al., 2018).

5 Conclusions

In the present study, we developed an integrated model framework for accurate multi-air-pollutant exposure assessments in high-density and high-rise cities. Following the proposed integrated model framework, with the air pollutant concentration data from a routine monitoring network, annual-average multi-air-pollutant exposure models for ambient PM_{10}, major PM_{10} chemical species, $PM_{2.5}$, NO_2, and O_3 were developed with relatively high predictive performance in Hong Kong, a typical high-rise high-density Asian city. The estimated air pollution maps (500 m × 500 m resolution) of these air pollutant mixtures could be used to support a unique combined exposure assessment in health studies.

We anticipate that the proposed integrated model framework can be easily extended to establish multi-air-pollutant exposure models in other cities. Apart from the LUR approach, other spatiotemporal statistical modelling methods, such as various machine learning algorithms, should be applied when a larger data set is available. Particularly, the development of high spatiotemporal exposure models should be explored when a high temporal-resolution air pollutant measurement data set is collected. Furthermore, the associations of combined exposure to multiple air pollutants with health endpoints should be analysed to provide new insights on the health-oriented air pollution control.

Data availability. The model data presented in this article are available from the authors upon request (steve.yim@ntu.edu.sg).

Author contributions. ZYL and SHLY designed the study. ZYL performed all the data analysis with support from SHLY. ZYL wrote the paper with contributions from all co-authors.

Competing interests. The authors declare that they have no conflict of interest.

Acknowledgements. We would like to thank the Hong Kong Environmental Protection Department and the Hong Kong Observatory for providing air quality and meteorological data, respectively.

Financial support. This work is funded by the Vice-Chancellor's Discretionary Fund of The Chinese University of Hong Kong (grant no. 4930744), the Dr. Stanley Ho Medicine Development Foundation (grant no. 8305509), and the project from the ENvironmental SUstainability and REsilience (ENSURE) partnership between the CUHK and UoE. ZYL was supported by the "100-top-talents Program" Start-up Grant of Sun Yat-sen University (Grant No. 220204).

References

Billionnet, C., Sherrill, D., and Annesi-Maesano, I.: Estimating the health effects of exposure to multi-pollutant mixture. Ann. Epidemiol. 22(2), 126-141, 2012.

Bowe, B., Xie, Y., Li, T., Yan, Y., Xian, H., and Al-Aly, Z.: The 2016 global and national burden of diabetes mellitus attributable to $PM_{2.5}$ air pollution. Lancet Planet. Health 2(7), e301-e312, 2018.

Brokamp, C., Jandarov, R., Rao, M.B., LeMasters, G., and Ryan, P.: Exposure assessment models for elemental components of particulate matter in an urban environment: A comparison of regression and random forest approaches. Atmos. Environ. 151, 1-11, 2017.

Burnett, R., Chen, H., Szyszkowicz, M., Fann, N., Hubbell, B., Pope, C.A., Apte, J.S., Brauer, M., Cohen, A., Weichenthal, S., and Coggins, J.: Global estimates of mortality associated with long-term exposure to outdoor fine particulate matter. Proc. Natl. Acad. Sci. U.S.A. 115(38), 9592-9597, 2018.

Cai, J., Ge, Y., Li, H., Yang, C., Liu, C., Meng, X., Wang, W., Niu, C., Kan, L., Schikowski, T., and Yan, B.: Application of land use regression to assess exposure and identify potential sources in $PM_{2.5}$, BC, NO_2 concentrations. Atmos. Environ. 223, 117267, 2020.

Chen, H., Zhang, Z., van Donkelaar, A., Bai, L., Martin, R.V., Lavigne, E., Kwong, J.C., and Burnett, R.T.: Understanding the joint impacts of fine particulate matter concentration and composition on the incidence and mortality of cardiovascular disease: A component-adjusted approach. Environ. Sci. Technol. 54(7), 4388-4399, 2020a.

Chen, J., de Hoogh, K., Gulliver, J., Hoffmann, B., Hertel, O., Ketzel, M., Weinmayr, G., Bauwelinck, M., van Donkelaar, A., Hvidtfeldt, U.A., and Atkinson, R.: Development of Europe-wide models for particle elemental composition using supervised linear regression and random forest. Environ. Sci. Technol. 54(24), 15698-15709, 2020b.

Chen, J., Rodopoulou, S., de Hoogh, K., Strak, M., Andersen, Z.J., Atkinson, R., Bauwelinck, M., Bellander, T., Brandt, J., Cesaroni, G., Concin, H.: Long-term exposure to fine particle elemental components and natural and cause-specific mortality—A pooled analysis of eight European cohorts within the ELAPSE project. Environ. Health Perspect. 129(4), 047009, 2021.

Coker, E., Liverani, S., Ghosh, J.K., Jerrett, M., Beckerman, B., Li, A., Ritz, B., and Molitor, J.: Multi-pollutant exposure profiles associated with term low birth weight in Los Angeles County. Environ. Int. 91, 1-13, 2016.

Cordioli, M., Pironi, C., De Munari, E., Marmiroli, N., Lauriola, P., and Ranzi, A.: Combining land use regression models and fixed site monitoring to reconstruct spatiotemporal variability of NO_2 concentrations over a wide geographical area. Sci. Total Environ. 574, 1075-1084, 2017.

Crouse, D.L., Peters, P.A., Hystad, P., Brook, J.R., van Donkelaar, A., Martin, R.V., Villeneuve, P.J., Jerrett, M., Goldberg, M.S., Pope III, C.A., and Brauer, M.: Ambient $PM_{2.5}$, O_3, and NO_2 exposures and associations with mortality over 16 years of follow-up in the Canadian Census Health and Environment Cohort (CanCHEC). Environ. Health Perspect. 123(11), 1180-1186, 2015.

Dominici, F., Peng, R.D., Barr, C.D., and Bell, M.L.: Protecting human health from air pollution: shifting from a single-pollutant to a multi-pollutant approach. Epidemiol. 21(2), 187-194, 2010.

Eeftens, M., Beelen, R., de Hoogh, K., Bellander, T., Cesaroni, G., Cirach, M., Declercq, C., Dėdelė, A., Dons, E., de Nazelle, A., and Dimakopoulou, K.: Development of land use regression models for $PM_{2.5}$, $PM_{2.5}$ absorbance, PM_{10} and PM_{coarse} in 20 European study areas; results of the ESCAPE project. Environ. Sci. Technol. 46(20), 11195-11205, 2012.

Eeftens, M., Meier, R., Schindler, C., Aguilera, I., Phuleria, H., Ineichen, A., Davey, M., Ducret-Stich, R., Keidel, D., Probst-Hensch, N., and Künzli, N.: Development of land use regression models for nitrogen dioxide, ultrafine particles, lung deposited surface area, and four other markers of particulate matter pollution in the Swiss SAPALDIA regions. Environmental Health 15(1), 53, 2016.

Eeftens, M., Odabasi, D., Flückiger, B., Davey, M., Ineichen, A., Feigenwinter, C., and Tsai, M.Y.: Modelling the vertical gradient of nitrogen dioxide in an urban area. Sci. Total Environ. 650, 452-458, 2019.

Fan, Z., Pun, V.C., Chen, X.C., Hong, Q., Tian, L., Ho, S.S.H., Lee, S.C., Tse, L.A., and Ho, K.F.: Personal exposure to fine particles ($PM_{2.5}$) and respiratory inflammation of common residents in Hong Kong. Environ. Res. 164, 24-31, 2018.

Gulliver, J., Morley, D., Dunster, C., McCrea, A., van Nunen, E., Tsai, M.Y., Probst-Hensch, N., Eeftens, M., Imboden, M., Ducret-Stich, R., and Naccarati, A.: Land use regression models for the oxidative potential of fine particles ($PM_{2.5}$) in five European areas. Environ. Res. 160, 247-255, 2018.

Han, H., Zhang, L., Liu, Z., Yue, X., Shu, L., Wang, X., and Zhang, Y.: Narrowing Differences in Urban and Nonurban Surface Ozone in the Northern Hemisphere Over 1990–2020, Environ. Sci. Technol. Lett., 10, 410–417, https://doi.org/10.1021/acs.estlett.3c00105, 2023.

HEI (Health Effects Institute): State of Global Air 2019. Special Report. Boston, MA, USA. Available at: https://www.stateofglobalair.org/sites/default/files/soga_2019_report.pdf (last accessed on February 2022), 2019.

Henderson, S.B., Beckerman, B., Jerrett, M., and Brauer, M.: Application of land use regression to estimate long-term concentrations of traffic-related nitrogen oxides and fine particulate matter. Environ. Sci. Technol. 41(7), 2422-2428, 2007.

HKEPD (Hong Kong Environmental Protection Department): Air quality in Hong Kong 2017. Available at: https://www.aqhi.gov.hk/api_history/english/report/files/AQR2017e_final.pdf (last accessed on February 2022), 2018.

HKEPD (Hong Kong Environmental Protection Department): Air quality in Hong Kong 2021. Available at: https://www.aqhi.gov.hk/api_history/english/report/files/AQR2021e_final.pdf (last accessed on August 2023), 2022.

HKO (Hong Kong Observatory): Climate of Hong Kong. Available at: http://www.hko.gov.hk/en/cis/climahk.htm# (last accessed on February 2022), 2020.

HKTD (Hong Kong Transport Department): Registered and licensing of vehicles by class of vehicles. Available at: https://www.td.gov.hk/en/transport_in_hong_kong/transport_figures/vehicle_registration_and_licensing/index.html (last accessed on February 2022), 2020.

Ho, C.C., Chan, C.C., Cho, C.W., Lin, H.I., Lee, J.H., and Wu, C.F.: Land use regression modeling with vertical distribution measurements for fine particulate matter and elements in an urban area. Atmos. Environ. 104, 256-263, 2015.

Hoek, G., Beelen, R., De Hoogh, K., Vienneau, D., Gulliver, J., Fischer, P., and Briggs, D.: A review of land-use regression models to assess spatial variation of outdoor air pollution. Atmos. Environ. 42(33), 7561-7578, 2008.

Hsu, C.Y., Wu, C.D., Hsiao, Y.P., Chen, Y.C., Chen, M.J., and Lung, S.C.C.: Developing land-use regression models to estimate $PM_{2.5}$-bound compound concentrations. Remote Sens. 10(12), 1971, 2018.

Huang, L., Zhang, C., and Bi, J.: Development of land use regression models for $PM_{2.5}$, SO_2, NO_2 and O_3 in Nanjing, China. Environ. Res. 158, 542-552, 2017.

Ji, W., Wang, Y., and Zhuang, D.: Spatial distribution differences in $PM_{2.5}$ concentration between heating and non-heating seasons in Beijing, China. Environ. Pollut. 248, 574-583, 2019.

Jin, L., Berman, J.D., Warren, J.L., Levy, J.I., Thurston, G., Zhang, Y., Xu, X., Wang, S., Zhang, Y., and Bell, M.L.: A land use regression model of nitrogen dioxide and fine particulate matter in a complex urban core in Lanzhou, China. Environ. Res. 177, 108597, 2019.

Jones, R.R., Hoek, G., Fisher, J.A., Hasheminassab, S., Wang, D., Ward, M.H., Sioutas, C., Vermeulen, R., and Silverman, D.T.: Land use regression models for ultrafine particles, fine particles, and black carbon in southern California. Sci. Total Environ. 699, 134234, 2020.

Lee, M., Brauer, M., Wong, P., Tang, R., Tsui, T.H., Choi, C., Cheng, W., Lai, P.C., Tian, L., Thach, T.Q., and Allen, R.: Land use regression modelling of air pollution in high density high rise cities: A case study in Hong Kong. Sci Total Environ. 592, 306-315, 2017.

Levy, I., Mihele, C., Lu, G., Narayan, J., and Brook, J.R.: Evaluating multipollutant exposure and urban air quality: pollutant interrelationships, neighborhood variability, and nitrogen dioxide as a proxy pollutant. Environ. Health Perspect. 122(1), 65-72, 2014.

Li, Z., Fung, J.C., and Lau, A.K.: High spatiotemporal characterization of on-road $PM_{2.5}$ concentrations in high-density urban areas using mobile monitoring. Build. Environ.143, 196-205, 2018.

Li, Z., Ho, K.F., Dong, G., Lee, H.F., and Yim, S.H.L.: A novel approach for assessing the spatiotemporal trend of health risk from ambient particulate matter components: Case of Hong Kong. Environ. Res. 204, 111866, 2022.

Li, Z., Ho, K.F., Chuang, H.C., and Yim, S.H.L.: Development and intercity transferability of land-use regression models for predicting ambient PM_{10}, $PM_{2.5}$, NO_2 and O_3 concentrations in northern Taiwan. Atmos. Chem. Phys. 21, 5063–5078, 2021.

Li, Z., Yim, S.H.L., and Ho, K.F. High temporal resolution prediction of street-level $PM_{2.5}$ and NO_x concentrations using machine learning approach. J. Clean. Prod. 268, 121975, 2020.

Liu, C., Henderson, B.H., Wang, D., Yang, X., and Peng, Z.R.: A land use regression application into assessing spatial variation of intra-urban fine particulate matter ($PM_{2.5}$) and nitrogen dioxide (NO_2) concentrations in City of Shanghai, China. Sci. Total Environ. 565, 607-615, 2016.

445   Lu, M., Soenario, I., Helbich, M., Schmitz, O., Hoek, G., van der Molen, M., and Karssenberg, D.: Land use regression models revealing spatiotemporal co-variation in NO_2, NO, and O_3 in the Netherlands. Atmos. Environ. 223, 117238, 2020.

Luminati, O., de Campos, B.L.D.A., Flückiger, B., Brentani, A., Röösli, M., Fink, G., and de Hoogh, K.: Land use regression modelling of NO_2 in Sao Paulo, Brazil. Environ. Pollut. 289, 117832, 2021.

450   Ma, M., Gao, Y., Ding, A., Su, H., Liao, H., Wang, S., Wang, X., Zhao, B., Zhang, S., Fu, P., and Guenther, A.B.: Development and Assessment of a High-Resolution Biogenic Emission Inventory from Urban Green Spaces in China. Environ. Sci. Technol. 56(1), 175-184, 2021.

Ma, X., Longley, I., Gao, J., Kachhara, A., and Salmond, J.: A site-optimised multi-scale GIS based land use regression model for simulating local scale patterns in air pollution. Sci. Total Environ. 685, 134-149, 2019.

455   Masiol, M., Zíková, N., Chalupa, D.C., Rich, D.Q., Ferro, A.R., and Hopke, P.K.: Hourly land-use regression models based on low-cost PM monitor data. Environ. Res. 167, 7-14, 2018.

Mauderly, J.L., Burnett, R.T., Castillejos, M., Özkaynak, H., Samet, J.M., Stieb, D.M., Vedal, S., and Wyzga, R.E.: Is the air pollution health research community prepared to support a multipollutant air quality management framework?. Inhal. Toxicol. 22(sup1):1-19, 2010.

460   Meng, X., Chen, L., Cai, J., Zou, B., Wu, C.F., Fu, Q., Zhang, Y., Liu, Y., and Kan, H.: A land use regression model for estimating the NO_2 concentration in Shanghai, China. Environ. Res. 137, 308-315, 2015.

Meng, X., Fu, Q., Ma, Z., Chen, L., Zou, B., Zhang, Y., Xue, W., Wang, J., Wang, D., Kan, H., and Liu, Y.: Estimating ground-level PM_{10} in a Chinese city by combining satellite data, meteorological information and a land use regression model. Environ. Pollut. 208, 177-184, 2016.

465   Miri, M., Ghassoun, Y., Dovlatabadi, A., Ebrahimnejad, A., and Löwner, M.O.: Estimate annual and seasonal PM_1, $PM_{2.5}$ and PM_{10} concentrations using land use regression model. Ecotoxicol. Environ. Saf. 174, 137-145, 2019.

Naughton, O., Donnelly, A., Nolan, P., Pilla, F., Misstear, B.D., and Broderick, B.: A land use regression model for explaining spatial variation in air pollution levels using a wind sector based approach. Sci. Total Environ. 630, 1324-1334, 2018.

470   Rappazzo, K.M., Baxter, L., Sacks, J.D., Alman, B.L., Peterson, G.C.L., Hubbell, B., and Neas, L.: Exploration of PM mass, source, and component-related factors that might explain heterogeneity in daily $PM_{2.5}$-mortality associations across the United States. Atmos. Environ. 262, 118650, 2021.

Ren, Y., Qu, Z., Du, Y., Xu, R., Ma, D., Yang, G., Shi, Y., Fan, X., Tani, A., Guo, P., and Ge, Y.: Air quality and health effects of biogenic volatile organic compounds emissions from urban green spaces and the mitigation strategies. Environ.
475   Pollut. 230, 849-861, 2017.

Renzi, M., Forastiere, F., Schwartz, J., Davoli, M., Michelozzi, P., and Stafoggia, M.: Long-Term PM_{10} Exposure and Cause-Specific Mortality in the Latium Region (Italy): A Difference-in-Differences Approach. Environ. Health Perspect. 127(6), 067004, 2019.

Requia, W.J., Coull, B.A., and Koutrakis, P.: Evaluation of predictive capabilities of ordinary geostatistical interpolation,
480   hybrid interpolation, and machine learning methods for estimating $PM_{2.5}$ constituents over space. Environ. Res. 175, 421-433, 2019.

Ross, Z., Jerrett, M., Ito, K., Tempalski, B., and Thurston, G.D.: A land use regression for predicting fine particulate matter concentrations in the New York City region. Atmos. Environ. 41(11), 2255-2269, 2007.

Saha, P.K., Sengupta, S., Adams, P., Robinson, A.L., and Presto, A.A.: Spatial correlation of ultrafine particle number and
485   fine particle mass at urban scales: implications for health assessment. Environ. Sci. Technol. (15), 9295-9304, 2020.

Song, M., Zhao, X., Liu, P., Mu, J., He, G., Zhang, C., Tong, S., Xue, C., Zhao, X., Ge, M., Mu, Y., 2023. Atmospheric NO_x oxidation as major sources for nitrous acid (HONO). npj Clim. Atmos. Sci. 6(1), 30.

Stafoggia, M., Breitner, S., Hampel, R., and Basagaña, X.: Statistical approaches to address multi-pollutant mixtures and multiple exposures: the state of the science. Curr. Environ. Health Rep. 4(4), 481-490, 2017.

490 Tang, R., Tian, L., Thach, T.Q., Tsui, T.H., Brauer, M., Lee, M., Allen, R., Yuchi, W., Lai, P.C., Wong, P., and Barratt, B.: Integrating travel behavior with land use regression to estimate dynamic air pollution exposure in Hong Kong. Environ. Int. 113, 100-108, 2018.

Vedal, S., and Kaufman, J.D.: What does multi-pollutant air pollution research mean?. Am. J. Respir. Crit. Care Med. 183(1), 4-6, 2011.

495 Wang, C., Cai, J., Chen, R., Shi, J., Yang, C., Li, H., Lin, Z., Meng, X., Liu, C., Niu, Y., and Xia, Y.: Personal exposure to fine particulate matter, lung function and serum club cell secretory protein (Clara). Environ. Pollut. 225, 450-455, 2017.

Wang, J., Cohan, D.S., and Xu, H.: Spatiotemporal ozone pollution LUR models: Suitable statistical algorithms and time scales for a megacity scale. Atmos. Environ. 237, 117671, 2020.

Wang, J., Wang, W., Zhang, W., Wang, J., Huang, Y., Hu, Z., Chen, Y., Guo, X., Deng, F., and Zhang, L.: Co-exposure to
500 multiple air pollutants and sleep disordered breathing in patients with or without obstructive sleep apneas: A cross-sectional study. Environ. Res. 212, 113155, 2022a.

Wang, Y., Xiao, S., Zhang, Y., Chang, H., Martin, R.V., Van Donkelaar, A., Gaskins, A., Liu, Y., Liu, P., and Shi, L.: Long-term exposure to $PM_{2.5}$ major components and mortality in the southeastern United States. Environ. Int. 158, 106969, 2022b.

505 WHO (World Health Organization): WHO global air quality guidelines: particulate matter ($PM_{2.5}$ and PM_{10}), ozone, nitrogen dioxide, sulfur dioxide and carbon monoxide. Available at: https://apps.who.int/iris/handle/10665/345329 (last accessed on February 2022), 2021.

Wolf, K., Cyrys, J., Harciníková, T., Gu, J., Kusch, T., Hampel, R., Schneider, A., and Peters, A.: Land use regression modeling of ultrafine particles, ozone, nitrogen oxides and markers of particulate matter pollution in Augsburg,
510 Germany. Sci. Total Environ. 579, 1531-1540, 2017.

Wu, H., Reis, S., Lin, C., and Heal, M.R.: Effect of monitoring network design on land use regression models for estimating residential NO_2 concentration. Atmos. Environ. 149, 24-33, 2017.

Xu, M., Sbihi, H., Pan, X., and Brauer, M.: Local variation of $PM_{2.5}$ and NO_2 concentrations within metropolitan Beijing. Atmos. Environ. 200, 254-263, 2019.

515 Xue, T., Zheng, Y., Li, X., Liu, J., Zhang, Q., and Zhu, T.: A component-specific exposure–mortality model for ambient $PM_{2.5}$ in China: findings from nationwide epidemiology based on outputs from a chemical transport model. Faraday Discuss. 226, 551-568, 2021.

Yim, S.H., Fung, J.C.H., Lau, A.K.H., and Kot, S.C.: Air ventilation impacts of the "wall effect" resulting from the alignment of high-rise buildings. Atmos. Environ. 43(32), 4982-4994, 2009.

520 Yim, S.H., Huang, T., Ho, J.M., Lam, A.S., Yau, S.T., Yuen, T.W., Dong, G.H., Tsoi, K.K., and Sung, J.J.: Rise and fall of lung cancers in relation to tobacco smoking and air pollution: A global trend analysis from 1990 to 2012. Atmos. Environ. 269, 118835, 2022.

Yim, S.H.L.: Development of a 3D real-time atmospheric monitoring system (3DREAMS) using Doppler LiDARs and applications for long-term analysis and hot-and-polluted episodes. Remote Sens. 12(6), 1036, 2020.

525 Yim, S.H.L., Wang, M., Gu, Y., Yang, Y., Dong, G., and Li, Q.: Effect of urbanization on ozone and resultant health effects in the Pearl River Delta region of China. J. Geophys. Res. Atmos. 124(21), 11568-11579, 2019.

Zeng, L., Yang, J., Guo, H., Lyu, X.: Impact of NOx reduction on long-term surface ozone pollution in roadside and suburban Hong Kong: Field measurements and model simulations. Chemosphere 302, 134816, 2022.

Zhang, J.J., Sun, L., Barrett, O., Bertazzon, S., Underwood, F.E., and Johnson, M.: Development of land-use regression
530 models for metals associated with airborne particulate matter in a North American city. Atmos. Environ. 106, 165-177, 2015.

Table 1. Pearson correlation coefficients (PCCs) among the LUR estimated concentration of ambient PM_{10}, PM_{10} TC, PM_{10} NO_3^-, PM_{10} SO_4^{2-}, PM_{10} Cd, $PM_{2.5}$, NO_2, and O_3 in Hong Kong.

	PM_{10}	PM_{10} TC	PM_{10} NO_3^-	PM_{10} SO_4^{2-}	PM_{10} Cd	$PM_{2.5}$	NO_2	O_3
PM_{10}	1	0.397**	0.589**	0.189**	0.430**	0.781**	0.570**	-0.354**
PM_{10} TC		1	0.747**	0.418**	0.432**	0.598**	0.785**	-0.677**
PM_{10} NO_3^-			1	0.495**	0.479**	0.729**	0.921**	-0.654**
PM_{10} SO_4^{2-}				1	0.192**	0.256**	0.488**	-0.383**
PM_{10} Cd					1	0.368**	0.522**	-0.174**
$PM_{2.5}$						1	0.696**	-0.500**
NO_2							1	-0.678**
O_3								1

** Correlation is significant at the 0.01 level (2-tailed).

535

Table 2. A comparison of this study with previous LUR studies. The example LUR studies focusing on at least one of the criteria air pollutants published in recent five years were included.

Study area	PM_{10}	PM_{10} TC	PM_{10} NO_3^-	PM_{10} SO_4^{2-}	PM_{10} Cd	$PM_{2.5}$	NO_2	O_3	References
Hong Kong, China	0.92	0.94	0.93	0.97	0.92	0.91	0.96	0.92	This work
Beijing, China						0.86			Xu et al. (2019)
Tianjin, China								0.98	Wang et al. (2020)
Nanjing, China						0.75	0.87	0.65	Huang et al. (2017)
Lanzhou, China						0.77	0.71		Jin et al. (2019)
Hong Kong, China						0.59	0.46		Lee et al. (2017)
Southern California, USA						0.47			Jones et al. (2020)
Sabzevar, Iran	0.75					0.71			Miri et al. (2019)
Auckland, New Zealand							0.66		Ma et al. (2019)
Mexico City, Mexico	0.73					0.83	0.81		Son et al. (2018)
Augsburg, Germany	0.91					0.84	0.95	0.92	Wolf et al. (2017)
Manchester, UK	0.95								Mölter and Lindley (2021)
Sydney, Australia							0.84		Cowie et al. (2017)
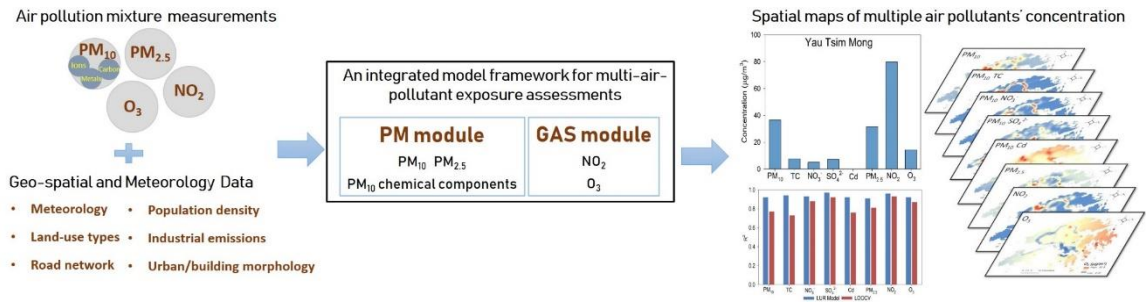
540 Figure 1. An integrated model framework for multi-air-pollutant exposure assessments in high-density cities. It mainly includes two components of particulate matters (PM module) and gaseous pollutants (GAS module). PM module consists of the measurement and LUR modelling of $PM_{2.5}$, PM_{10}, and PM_{10} major chemical components (e.g., ions, metals, and carbon), while GAS module involves the measurement and LUR modelling of NO_2 and O_3.
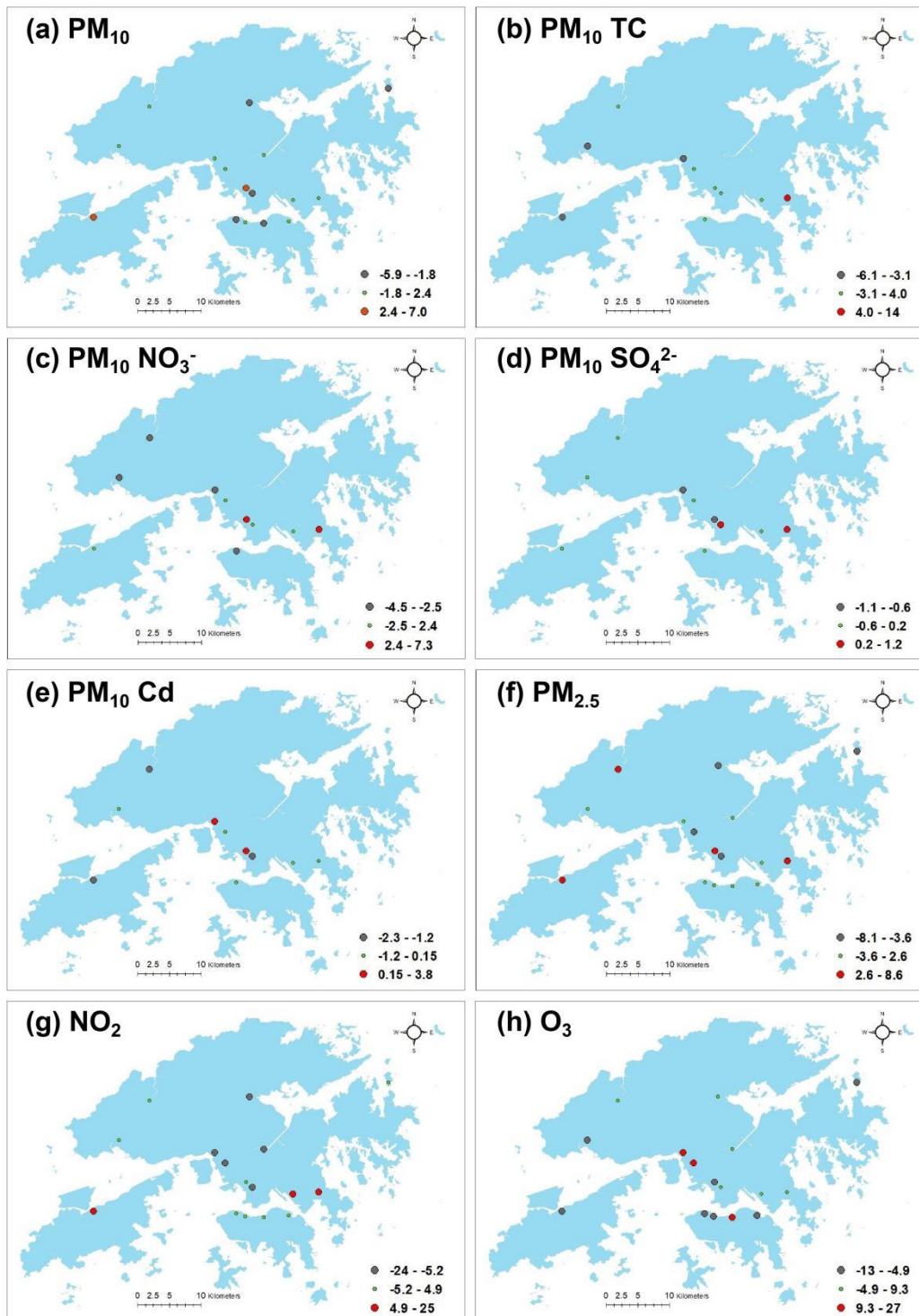
545 Figure 2. The distribution of prediction error fractions (%) of the established LUR models. The prediction error fraction is defined as [(predicted concentration – observed concentration)/observed concentration].
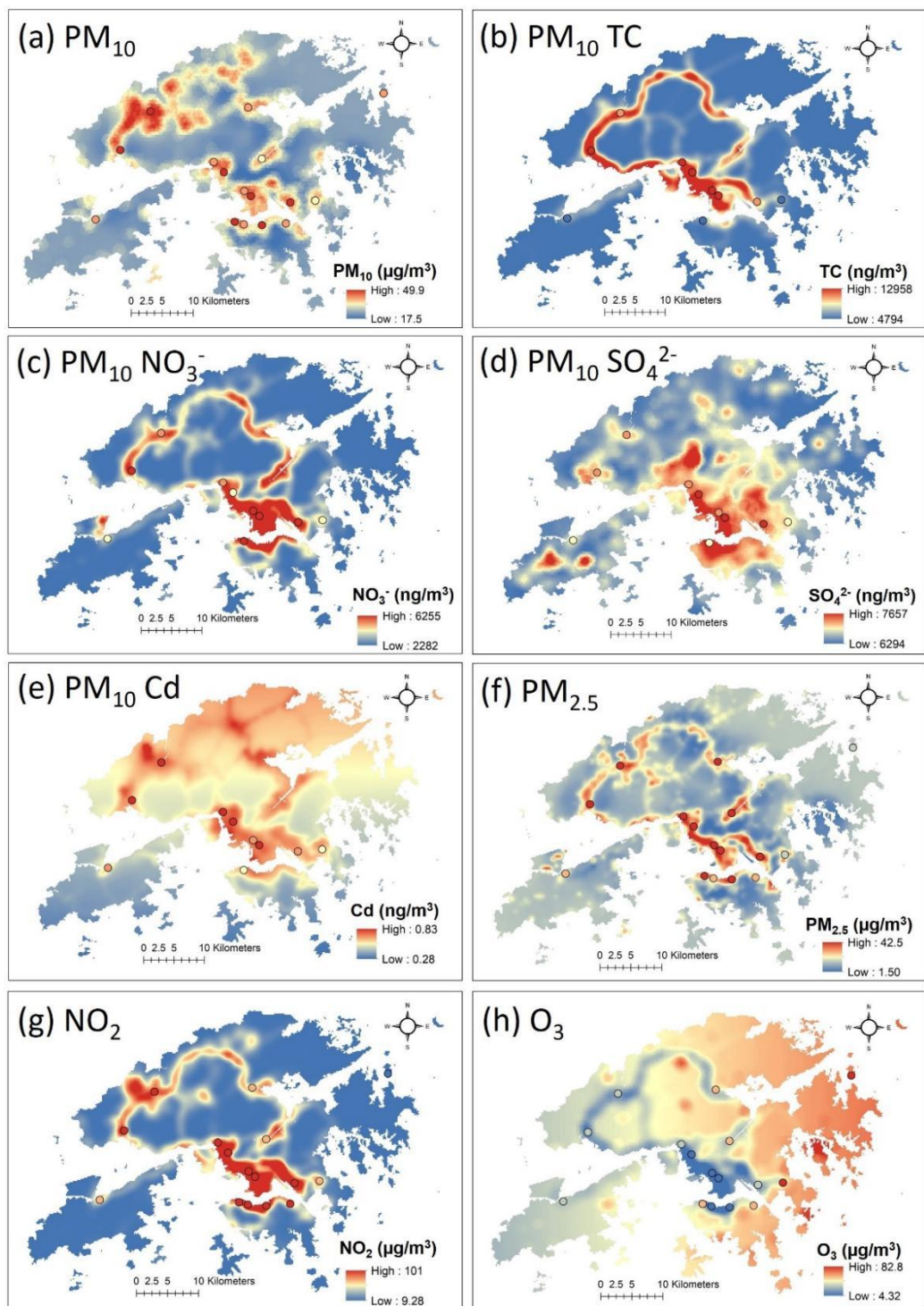
Figure 3. LUR model-derived spatial distribution maps of annual-average ambient PM$_{10}$, PM$_{10}$ TC, PM$_{10}$ NO$_3^-$, PM$_{10}$ SO$_4^{2-}$, PM$_{10}$ Cd, PM$_{2.5}$, NO$_2$, and O$_3$ concentration in Hong Kong. The colored circles represent observations at AQMSs.

550
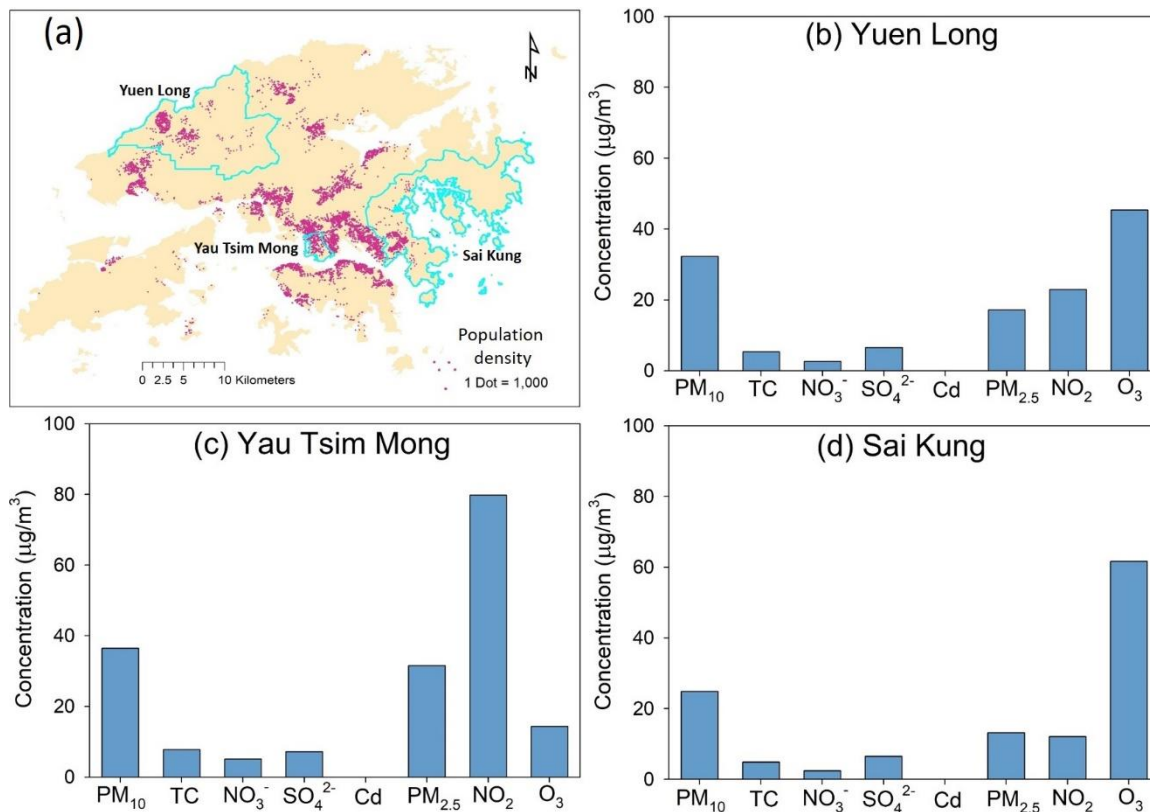
Figure 4. The average LUR estimated ambient PM_{10}, PM_{10} TC, PM_{10} NO_3^-, PM_{10} SO_4^{2-}, PM_{10} Cd, $PM_{2.5}$, NO_2, and O_3 concentration in three representative districts in Hong Kong. (a) The distribution of Yuen Long, Yau Tsim Mong, and Sai Kung districts in Hong Kong with the population density shown. (b) Yuen Long (a district more influenced by the transboundary pollution). (c) Yau Tsim Mong (a high-density district more influenced by vehicular emissions). (d) Sai Kung (a rural district).